Influence of thermal relaxation and ion bombardment on the electronic properties of amorphous SiAu films

Influence of thermal relaxation and ion bombardment on the electronic properties of amorphous SiAu films

H-G Boyen†, P Rieger†, P Häussler†, F Baumann†, G Indlekofer‡, P Oelhafen‡ and H-J Güntherodt‡

† Physikalisches Institut, Universität Karlsruhe, PO Box 6380, 75 Karlsruhe 1, Federal Republic of Germany
‡ Institut für Physik, Universität Basel, Klingelbergstrasse 82, 4056 Basel, Switzerland

Abstract. Effects of thermal relaxation on amorphous SiAu films are investigated by means of photoelectron spectroscopy and measurements of the electrical resistivity and specific heat. Annealing of the films in the amorphous state increases the resistivity and reduces the electronic density of states at the Fermi energy. These relaxation effects can be reversed by irradiation with 5 keV argon ions at low temperature. The results are discussed in the framework of structural relaxation, clustering and a scaling theory given by McMillan.

1. Introduction

Annealing of amorphous solids well below their crystallisation temperature usually changes many of their physical properties. These changes are attributed to a structural relaxation, i.e. to a rearrangement of the atoms to more stable configurations within the amorphous state or to clustering. In disordered metals the relation between the atomic structure and the electronic density of states (DOS) has been subject of many theoretical investigations [1]. Whenever there is a peak in the structure function at lattice vectors K_p where the band-gap coefficient $2|v(K_p)|$ is finite, a minimum in the density of states at the corresponding energy should occur [1, 2]. For amorphous noble-metal/simple-metal alloys this structure-induced effect on the DOS has been shown experimentally [3]. Correlations between structure and electronic properties of amorphous metals, e.g. between the resistivity and the electronic density of states at the Fermi energy E_F are reported [4]. These correlations were found by studying the alloys as a function of composition. In the present work we investigate how the electronic properties of amorphous SiAu (a-SiAu) change when their atomic structure is changed by annealing (decreasing disorder) and by successive ion bombardment (increasing disorder). Under certain circumstances annealing and irradiation are inverse processes. Ultraviolet photoelectron spectroscopy (UPS) and specific heat measurements were performed to get detailed information about the DOS near E_F. Simultaneously, resistivity measurements were performed to observe the effect of annealing or irradiation on transport properties. We correlate the UPS data with the resistivity data and discuss them in the light of structural relaxation, clustering and a scaling theory, including localisation and electron–electron interaction [5].

2. Some experimental details

The photoemission measurements were performed with a commercial spectrometer (Leybold EA10-100). The samples were prepared *in situ* by sequentially flash evaporating small amounts of SiAu pellets onto a quartz substrate held at 77 K. The pressure during condensation was typically 2×10^{-8} mbar. UPS ($h\nu = 21.2$ eV) was used to investigate the valence-band structure, XPS ($h\nu = 1253.6$ eV) to check the composition of the alloys. In the UPS spectra no significant contaminations could be detected, especially no oxygen. Contributions of about 5 at.% oxygen and copper seen in the XPS spectra come exclusively from the sample holder as shown later by experiments using larger film cross sections. All spectra were taken at 77 K and corrected for satellite contributions [4]. The films were subsequently annealed *in situ* at temperatures T_a well below their crystallisation temperatures. a-$Si_{70}Au_{30}$ was irradiated stepwise at 77 K with 5 keV Ar^+ ions. The total fluence after the last step of irradiation was 5×10^{14} Ar^+ cm^{-2}. The heat capacity of another a-$Si_{70}Au_{30}$ -sample, prepared *in situ* in a ^{3}He-cryostat at a condensation temperature of 100 K, was determined between 0.3 K $< T < 5.0$ K in the as-quenched state and after different steps of annealing. The specific heat measurement was performed with an AC heating method [7].

3. Results

Figure 1 shows the UPS spectra of a-$Si_{70}Au_{30}$ for different states of annealing with an additional enlargement at small binding energies. Apart from satellite corrections, no data processing, e.g. subtraction of the inelastic background or normalisation, has been performed. At binding energies of 4.8 and 6.7 eV two distinct peaks occur due to the Au 5d valence states. These peaks have a very similar shape to those observed in the liquid phase [7]. With increasing annealing temperature T_a two effects occur. There is a decrease of the Au $5d_{5/2}$ peak, which is not discussed in this paper, and furthermore there is a decrease of the intensity close to E_F accompanied by an increase of the resistance (see the inset of figure 1). The numbers indicate corresponding states of annealing.

In order to show the influence of annealing more quantitatively, we plot in figure 2(a) for several alloys $I_i(E_F)$, the intensity of the spectra at E_F after annealing, normalised to $I_0(E_F)$, the intensity of the as-quenched samples, as a function of T_a. Obviously the change of intensity at E_F is largest for the silicon-rich alloys. Figure 2(b) shows the corresponding resistivities measured at 77 K and normalised to the values in the as-quenched state. The resistivity increases monotonically with T_a and again the silicon-rich alloys show the most pronounced changes.

Valence-band spectra of disordered alloys are usually interpreted in terms of the density of states [8]. In order to test whether the decrease of the spectra near E_F really reflects a change of the DOS, we performed specific-heat measurements on a-$Si_{70}Au_{30}$. Figure 3 shows these data as a function of temperature for various states of annealing. Disregarding the increase below 0.5 K, due to the onset of superconductivity, from the linear contribution we calculate $N(E_F)$ which decreases with increasing T_a. These data normalised to $N_0(E_F)$ of the as-quenched state are included in figure 2(a) as open symbols. Obviously the relative changes of $N(E_F)$ are quantitatively in good agreement with those of $I(E_F)$. We conclude from this that the UPS spectra near E_F indeed reflect the DOS. In this analysis we made two assumptions. Firstly we neglected
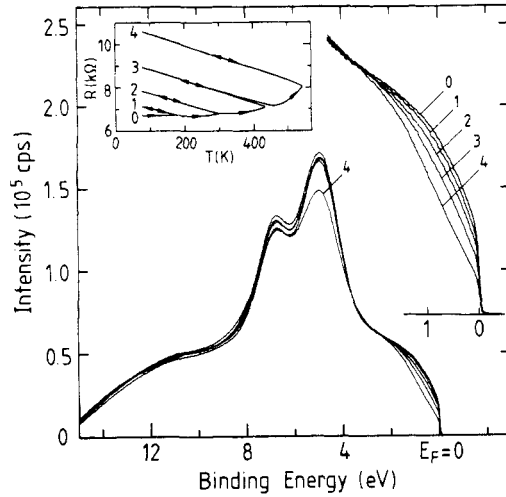
Figure 1. UPS-spectra of a-$Si_{70}Au_{30}$ after annealing to various temperatures T_a: 0, as-quenched; 1, 172 K; 2, 300 K; 3, 430 K; 4, 538 K. The spectra near E_F are shown enlarged. Inset: resistance versus temperature.
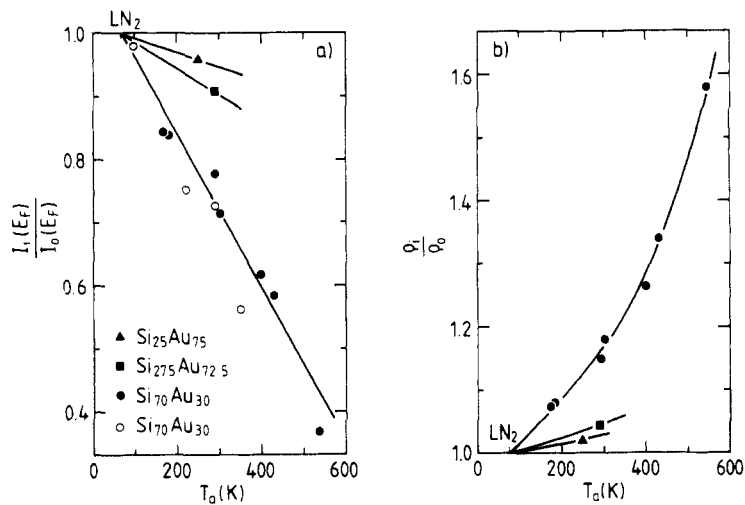
Figure 2. (a) Normalised intensity of the UPS spectra at E_F versus T_a; open symbols represent the normalised electronic density of states at E_F as deduced from specific heat measurements. (b) Normalised resistivity versus T_a.

the electron–phonon enhancement in the specific-heat data which may be substantial. However, in the normalised DOS only changes of this enhancement due to annealing would be effective. Secondly we neglect contributions from two-level systems that are very small in some amorphous metals [9] but strongly concentration dependent and quite large in others [10].

Figure 4 shows the normalised DOS at E_F versus the normalised conductivity for the three different alloys at 77 K. Although there is a linear relation between the two parameters it is important to note that there is no proportionality, which will be
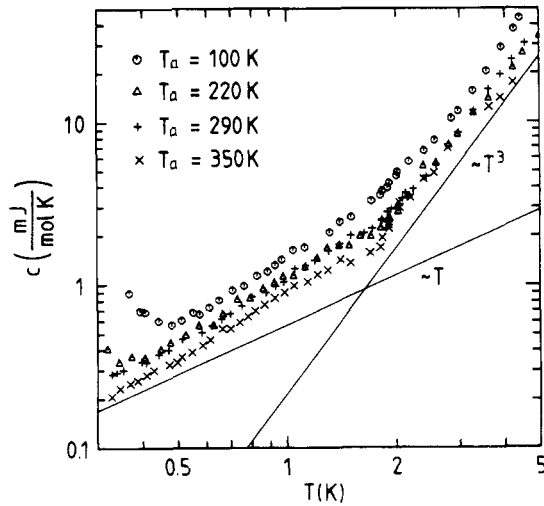
Figure 3. Specific heat of a-Si$_{70}$Au$_{30}$ versus T for various temperatures of annealing.
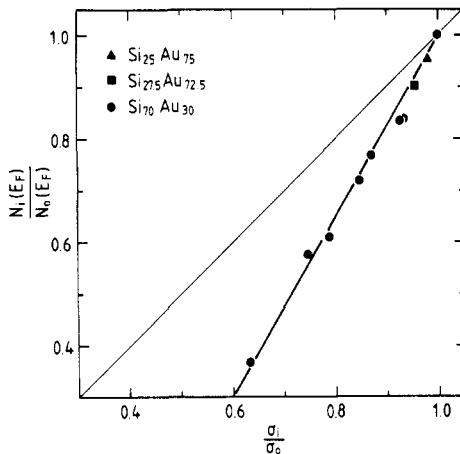

Figure 4. Normalised DOS at E_F versus normalised conductivity at 77 K. The thin line indicates $N(E_F) \propto \sigma$.

discussed below.

The sample shown in figure 1 (thickness $d = 16$ nm) has been irradiated at $T = 77$ K after the last step of annealing ($T_a = 538$ K) with Ar$^+$ ions as mentioned above. Monte-Carlo simulations [11] give a penetration depth of 4.7 nm for ions with the energy used in this experiment. Together with the total fluence of 5×10^{14} Ar$^+$ cm^{-2} we calculate two displacements per atom after the final step of irradiation. Figure 5 shows the valence band spectra as well as the corresponding resistance after each step. Obviously the DOS near E_F increases with irradiation time t_{irr} while the resistance decreases showing a saturation behavior. Obviously irradiation increases the disorder within the penetration depth as much as in the as-quenched state. This can be seen from the UPS spectra near E_F which are after irradiation nearly the same as after quenching. In contrast to UPS which is sensitive only to the
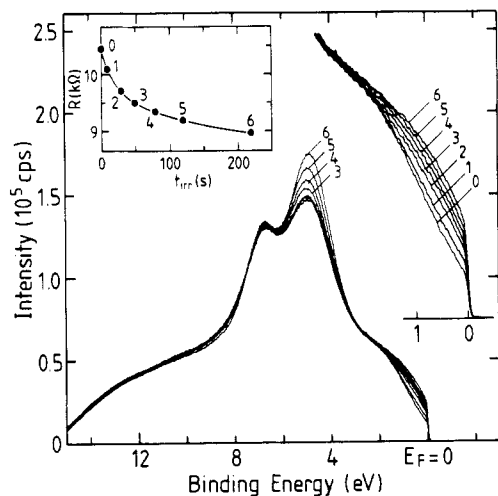
Figure 5. UPS spectra of a-Si70Au30 taken after relaxation and stepwise irradiation with 5 keV Ar$^+$ ions. Inset: the corresponding change of the resistance as a function of irradiation time t_{irr}. All data are taken at 77 K.
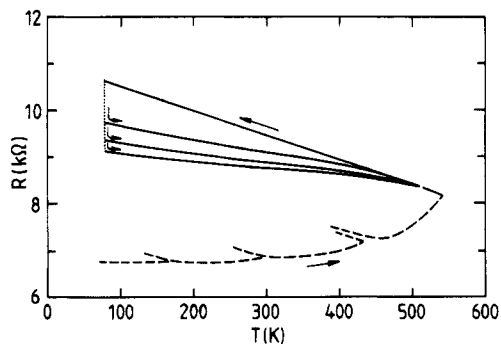
Figure 6. Resistance of a-Si70Au30 for several cycles of annealing and irradiation. Broken curves, first annealing process; dotted line, irradiation; straight lines, annealing up to 500 K and cooling down.

first atomic layers the electrical resistance of the films is sensitive to the whole volume of the samples. Because the film thickness is larger than the penetration depth, irradiation cannot decrease the resistance to the value measured just after quenching. However, the film resistance agrees very well with the resistance of a sandwich of an annealed film ($d = 11.3$ nm) covered with an as-quenched film ($d = 4.7$ nm). The whole process of annealing at 500 K, followed by subsequent stepwise irradiation with different total fluences was repeated twice. The resistance at 77 K, measured directly after each annealing at 500 K, stayed constant in all three cycles within an error of 1% (figure 6). Therefore sputtering effects, which lead to a decreasing thickness or an altered surface composition, can be neglected. Obviously in this experiment relaxation and ion bombardment are inverse processes.

4. Discussion

We have shown that annealing of a-SiAu causes a decrease of the DOS at E_F and an increase of the resistivity. Assuming a structural influence on the DOS as reported elsewhere [4] we would expect in simplest approximation that during annealing the maximum in the structure function close to $2k_F$ increases. This causes a decrease of the DOS at E_F accompanied with an increase of the covalent character of the bonds and an increase of resistivity. Unfortunately the effect of annealing on the structure function of a-SiAu in not known. In case of a-GeAu, which in many respects is similar to a-SiAu, the maximum at $2k_F$ slightly decreases due to annealing [12] in contrast to what we expected. As long as structural relaxation is not confirmed by structure investigations, other processes have to be considered also.

In a-GeAu similar changes of the resistivity are observed and a transition to the insulating state was reached by heat treatment of metallic samples [13]. This phenomenon was interpreted as the growth of small Au clusters, reducing the mean Au

concentration within the amorphous matrix. X-ray diffraction experiments supported this model [13]. A clustering of Au atoms may also occur in a-SiAu. Electron-diffraction measurements revealed microcrystallites of Au with a size of 2–3 nm [14]. Unfortunately the annealing temperatures were not reported. Similar irreversible changes of the resistivity of a-SiAu have been measured at temperatures below 77 K [15], which are difficult to understand in terms of clustering effects.

Hints for clustering in our samples come from the Au 5d states. In the as-quenched samples the Au $5d_{5/2}$ peak shifts as a function of Au content from $E_B = 4.4$ eV (a-$Si_{20}Au_{80}$) to $E_B = 5.2$ eV (a-$Si_{80}Au_{20}$). The annealing of a-$Si_{70}Au_{30}$ causes a slight shift of the Au-$5d_{5/2}$ peak to lower binding energies, not visible in figure 1. This shift may indicate a decrease of the Au content in the amorphous matrix, due to a clustering of Au atoms. The shift of the Au $5d_{5/2}$ peaks versus Au content in the as-quenched alloys allows an estimation of the effective composition of the amorphous matrix after annealing. Figure 7 shows the conductivity of the as-quenched samples (full squares) versus Au content in excellent agreement with data of Mangin *et al* [16] (full triangles). The full circles show the conductivity of a-$Si_{70}Au_{30}$ after annealing versus the effective Au concentration, estimated from the shift of the Au $5d_{5/2}$ peak. The agreement of these data with the results obtained on the as-quenched samples may support a clustering during annealing.
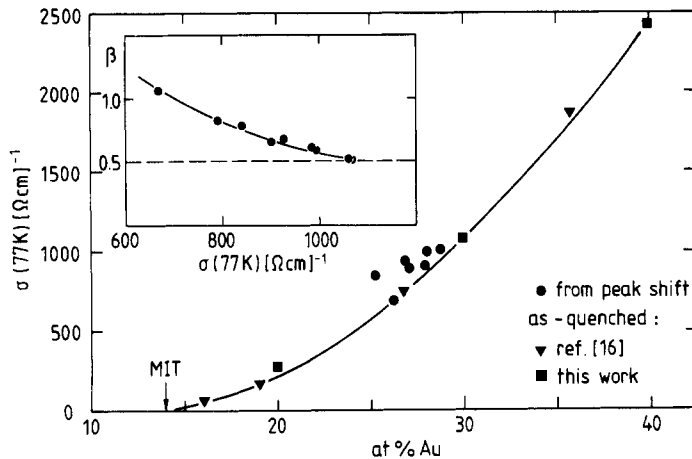

Figure 7. Conductivity of a-SiAu as a function of Au concentration. ■, ▼, as-quenched. The change of the conductivity and composition of a-$Si_{70}Au_{30}$ due to annealing is represented by ●. Inset: the exponent β in equation (2) versus the conductivity of $Si_{70}Au_{30}$.

The results plotted in figure 7 shows that the conductivity decreases with decreasing Au content and vanishes below 14 at.% Au, the critical Au concentration for the metal–insulator transition (MIT) of a-SiAu [14]. Although our samples are obviously not close to the MIT we discuss our results in the frame of the theory developed by McMillan [5]. This theory is based on scaling arguments and the assumption of the localisation of Coulomb interacting electrons in a random potential and for three-dimensional metallic systems gives

$$\sigma(T) = \sigma(0)[1 + (k_B T/\Delta)^{1/2}] \qquad \text{for } k_B T < \Delta \qquad (1)$$

$$N(E) = N(E_F)[1 + (E/\Delta)^{1/2}] \qquad \text{for } E < \Delta \qquad (2)$$

$$N(E_F) \sim \sigma(0)^{3-\eta} \tag{3}$$

$$\Delta \sim \sigma(0)^{\eta}. \tag{4}$$

Here $\sigma(0)$ is the conductivity at $T{=}0K$ and η and Δ denote a critical exponent and the energy width of an electron wave packet at the critical length scale.

For a wide variety of materials, including a-SiAu, the validity of (1) or (2) has been verified experimentally [17–21]. In all cases $\Delta \propto \sigma(0)^2$ was obtained [22–24], giving the universal value $\eta = 2$ (via (4)). According to (3) this has the interesting consequence that $N(E_F)$ should be proportional to $\sigma(0)$. This proportionality was indeed observed in a-SiNb [22] which fulfils all predictions of McMillan's theory.

In order to compare our data with (3) we need $\sigma(0)$. Because our measurements were performed at 77 K we measured for one a-Si$_{70}$Au$_{30}$ film $\sigma(T)$ down to $T = 1$ K and determined $\sigma(0)$ by extrapolation. For the various states of annealing we found

$$\frac{\sigma_i(0)}{\sigma_0(0)} \approx \frac{\sigma_i(T = 77 \text{ K})}{\sigma_0(T = 77 \text{ K})} \tag{5}$$

so the data at 77 K can be used as well as those at 0 K. As already shown in figure 4, there is *no* proportionality between $N(E_F)$ and $\sigma(0)$, in clear contradiction to the scaling theory.

In order to compare our data with (2) we made a fit of the valence-band spectra to the expression $N(E_B) = \alpha[1 + (E_B/\Delta)^{\beta}]$ for 1.5 eV $> E_B > 0$. Prior to the fit, the spectra were corrected for the energy dependence of the spectrometer transmission and for a non-linear background. For β we obtained the expected value $\beta \approx \frac{1}{2}$ only for the as-quenched samples with large σ shown in the inset of figure 7. However, for the annealed samples with smaller σ we found much higher values for β. But, even for the samples with $\beta \approx \frac{1}{2}$, significant discrepancies between our data and literature data occur. While our fit yields $\Delta \approx 0.12$ eV, measurements on many different materials all gave $\Delta \approx 2.5$ eV, a factor of about 20 higher [24]. Discrepancies of β and Δ were also reported for a-GeAu [21].

One of the basic assumptions in scaling theory is the homogeneity of the materials on a length scale larger than the critical length [5]. We conclude that our samples do not fulfil this requirement of the theory. Probably our samples are inhomogeous because of phase separation and/or clustering effects.

5. Summary

The combination of UPS with resistance and specific heat measurements is a powerful tool to study the electronic properties of amorphous metals. We used this combination to study annealing and irradiation effects of a-SiAu below the crystallisation temperature. Our measurements show that the UPS spectra of a-SiAu at E_F reflect the DOS. Annealing causes a decrease of the DOS at E_F and a decrease of the conductivity. Irradiation with Ar$^+$ ions at low temperatures is the inverse process of annealing. The annealing behaviour may be caused by clustering of Au as well as by structural relaxation. Our samples cannot be described by the scaling theory of McMillan because they do not seem to fulfil the assumptions made in the theory.

Acknowledgments

References

[1] Ballentine L A 1966 *Can. J. Phys.* **44** 2533; 1975 *J. Chem. Phys.* **31** 263
     Halder N C and Phillips K C 1983 *Phys. Status Solidi* b **115** 9
[2] Heine V and Weaire D 1970 *Solid State Physics, Advances in Research and Applications* vol 24, ed H Ehrenreich, F Seitz, and D Turnbull (New York: Academic) p 247
[3] Häussler P, Baumann F, Krieg J, Indlekofer G, Oelhafen P and Güntherodt H-J 1983 *Phys. Rev. Lett.* **51** 714
     Häussler P, Baumann F, Gubler U, Oelhafen P and Güntherodt H J 1988 *Z. Phys. Chem., NF* **157** 471
[4] Häussler P 1990 *Glassy Metals III (Topics in Applied Physics)* ed H Beck and H-J Güntherodt (Berlin: Springer) submitted
[5] McMillan W L 1981 *Phys. Rev.* B **24** 2739
[7] Sullivan P F and Seidel G 1968 *Phys. Rev.* **173** 679
[7] Indlekofer G, Oelhafen P, Güntherodt H-J, Hague C F and Mariot J-M 1988 *Z. Phys. Chem., NF* **157** 575
[8] Oelhafen P 1987 *Amorphous and Liquid Materials (NATO ASI series E 118)* ed E Lüscher *et al* (Dordrecht: Martinus Nijhoff) pp 333-44
[9] Sürgers C and von Löhneysen H 1988 *Z. Phys.* B **70** 361
[10] Rieger P and Baumann F 1990 *J. Phys.: Condens. Matter* submitted
[11] Biersack J P and Haggmark L G 1980 *Nucl. Instrum. Methods* **174** 257
[12] Krapp M, Lambrecht A and Hasse J 1985 *Z. Phys.* B **61** 167
     Krapp M 1984 Diploma work, Physikalisches Institut, Universität Karlsruhe (unpublished)
[13] Osofsky M, Tardy H, LaMadrid M and Mochel J M 1985 *Phys. Rev.* B **32** 2101
[14] Kishimoto N and Morigaki K 1979 *J. Phys. Soc. Japan* **46** 497
[15] Möckel D 1975 *PhD Thesis* Universität Karlsruhe
[16] Mangin P, Marchal G, Mourey C and Janot C 1980 *Phys. Rev.* B **21** 3047
[17] Yamaguchi M, Nishida N, Furubayashi T, Morigaki K, Ishimoto H and Ono K 1983 *Physica* **117–118** 694
[18] Nishida N, Yamaguchi M, Furubayashi T, Morigaki K, Ishimoto H and Ono K 1982 *Solid State Commun.* **44** 305
[19] Nishida N, Furubayashi T, Yamaguchi M, Shinohara M, Miura Y, Takano Y, Morigaki K, Ishimoto H and Ono K 1983 *J. Non-Cryst. Solids* **59–60** 149
[20] Furubayashi T, Nishida N, Yamaguchi M, Morigaki K and Ishimoto H 1985 *Solid State Commun.* **55** 513
[21] Furubayashi T, Nishida N, Yamaguchi M, Morigaki K and Ishimoto H 1986 *Solid State Commun.* **58** 587
[22] Hertel G, Bishop D J, Spencer E G, Rowell J M and Dynes R C 1983 *Phys. Rev. Lett.* **50** 743
[23] Cochrane R W and Ström-Olsen J O 1984 *Phys. Rev.* B **29** 1088
[24] Löbl P, Esguerra M, Küss F, Lüscher E, Fritsch G, von Allmen M, Kambli U and Schulte A 1987 *Solid State Commun.* **64** 1107